Rydberg states and spin-orbit coupling of the thallium atom

King-Chuen Lin* and Hsi-Chieh Lee
Department of Chemistry, National Taiwan University, Taipei, Taiwan, Republic of China
and Institute of Atomic and Molecular Sciences, Academia Sinica, P.O. Box 23-166, Taipei, Taiwan 10764, Republic of China

Arepalli Sivaram
Lockheed Engineering and Sciences Company, Houston, Texas 77058-3711
(Received 25 February 1992)

Using the resonance-enhanced multiphoton-ionization technique, we have identified the $n\,^2P_{1/2}(7 \le n \le 20)$, $n\,^2P_{3/2}(7 \le n \le 23)$, and $n\,^2F_{5/2,7/2}(5 \le n \le 21)$ Rydberg states following photodissociation of TlI. The $n\,^2P_{1/2,3/2}$ spin-orbit splitting can be resolved and well compared to its theoretical counterpart with an accuracy of $\pm 3.5\%$. In terms of photoionization-cross-section prediction, we have also satisfactorily interpreted the discrepancy for the relative ionization intensity, via the respective intermediate $n\,^2P_{3/2}$ and $n\,^2P_{1/2}(n \le 11)$ doublets, from their statistical weight.

PACS number(s): 32.80.Rm, 32.80.Fb

I. INTRODUCTION

The resonance-enhanced multiphoton-ionization (REMPI) technique has been widely employed to probe the high-lying states of an atom or a molecule, and thereby numerous new states are identified [1,2]. These Rydberg states are difficult to probe with conventional optical spectroscopy. For detecting a high-lying atom, for instance, the fluorescence method will become less sensitive with increase of principal quantum number n, since the transition oscillator strength varies in proportion to n^{-3} [1], while REMPI can feasibly ionize the excited atoms and monitor the resulting ions with a detection efficiency close to unity. Therefore, in this paper we attempt to employ this technique to characterize the Rydberg states of Tl atoms, which will result from the photodissociation of TlI. Mirza and Duley have also conducted a similar REMPI experiment with pure Tl sample, and identified the Tl nP and nF Rydberg states up to $n=21$ and 20, respectively [3]. However detailed work on the resolution of the $n\,^2P_{1/2}$ and $n\,^2P_{3/2}$ spin-orbit splitting and the characterization of their relative intensity in the ionization process has not yet occurred. This motivates us to carry out this experiment.

In our work, a Nd:YAG (where YAG denotes yttrium aluminum garnet) laser-pumped dye laser has been employed to produce Tl $(6\,^2P_{1/2})$ and Tl*$(6\,^2P_{3/2})$ fragments following a one- or two-photon dissociation of TlI, and subsequently to ionize these atoms through their intermediate nP or nF Rydberg states by a $(2+1)$-REMPI process. In this manner, we have identified the $n\,^2P_{1/2}(7 \le n \le 20)$, $n\,^2P_{3/2}(7 \le n \le 23)$, and $n\,^2F_{5/2,7/2}(5 \le n \le 21)$ Rydberg series, and have resolved the spin-orbit couplings for the nP fine-structure states; the latter splittings are satisfactorily compared to their theoretical counterparts based on a one-valence-electron, single-configuration model. Finally, in terms of the ionization-cross-section prediction, we have interpreted the relative intensity for the ionization process via the intermediate $n\,^2P_{1/2}$ and $n\,^2P_{3/2}$ doublets.

II. EXPERIMENT

The reagent TlI, from purchase without further purification, was deposited in the finger reservoir of a six-armed quartz cell, which was enclosed in a firebrick oven. Through the top arm, the cell was connected to a vacuum line and evacuated below 10^{-5} Torr before operation. The temperature of the cell body was maintained around 593–633 K with an accuracy of ± 2 K, about 80 K higher than that of the sample reservoir to prevent the TlI vapor from condensing onto the windows. The resultant TlI vapor pressure corresponded to 10^{-4}–10^{-3} Torr (or 3×10^{12}–2×10^{13} cm^{-3}) [4], and the number density of the fragmented Tl was estimated to be 10^{10}–10^{11} cm^{-3} [5]. A similar oven design as in this work has been reported in detail elsewhere [6,7].

As a radiation source for conducting both photodissociation and ionization processes, a Nd:YAG laser-pumed dye laser, having a bandwidth of 0.025 nm at 400 nm, a pulse duration of 5–8 nsec, and a repetition rate of 10 Hz was tuned ranging from 600 to 280 nm. The uv-wavelength portion was accessible through the operation of a frequency-doubled potassium dihydrogen phosphate (KDP) crystal device. The laser energy varied from 1–30 mJ throughout the experiment. Following photodissociation of the TlI, the focused, impinging laser beam can then successively ionize the fragmented Tl atoms through a selective intermediate nP or nF Rydberg state. The multiphoton-ionization process was considered to dominate over the other ionization processes in our case with a TlI vapor pressure as low as 10^{-3}–10^{-4} Torr [8]. However, when n increases, the energy defect between the Rydberg states $(n > 14)$ and the ionization threshold becomes smaller than the thermal energy kT. Thus the contribution of the thermal ionization may then become significant.

The produced Tl^+ ions were collected with a pair of voltage-biased nichrome probes, which were set about 1 cm apart. The ion current was amplified with a current amplifier prior to input to a boxcar integrator for signal

processing. The resulting ion signal was displayed on an oscilloscope or stored in a microcomputer for further analysis.

III. RESULTS AND DISCUSSION

A. Rydberg state identification

The Rydberg states of Tl atoms, as fragmented to the ground or spin-orbit excited states following photodissociation of TlI, were probed using a (2+1)-REMPI technique. A portion of the ionization spectra is shown in Fig. 1. The $n\,^2P_{1/2}(7 \le n \le 20)$, $n\,^2P_{3/2}(7 \le n \le 23)$, and $n\,^2F(5 \le n \le 21)$ Rydberg series are identified; the results, which are compared well to those reported elsewhere [3,9], are listed in Table I.

The term energies obtained can be essentially characterized using the Rydberg formula [1,2]. By taking the derivative of the formula with respect to the principal quantum number n, one obtains

$$\frac{dE_n}{dn} = \frac{2\mathcal{R}}{(n-\delta)^3} , \tag{1}$$

where $\mathcal{R}$ is the Rydberg constant, δ is the quantum defect, and $n-\delta$ denotes the effective principal quantum number which can be related to the term energy E_n by the expression

$$n-\delta = n^* = Z_a/E_n^{1/2} . \tag{2}$$

For a neutral atom, the charge of the atomic core Z_a is equal to unity. As n becomes large, the left-hand side of Eq. (1) can be replaced by $\Delta E_n/\Delta n$ approximately; ΔE_n is the term energy difference between two successive states. The resulting log-scale plot of $\Delta E_n/\Delta n$ for the $n\,^2P_{1/2}$, $n\,^2P_{3/2}$, and $n\,^2F$ Rydberg series against n^{*3} is shown in Fig. 2; the slope is measured to be -1, indicating that the Rydberg state assignment should be reliable. Especially for large n, the term energy can be well characterized by Eq. (1). The values of n^* and δ as functions of n are also listed in Table II. As expected, the n dependence of δ is found to be invariant.

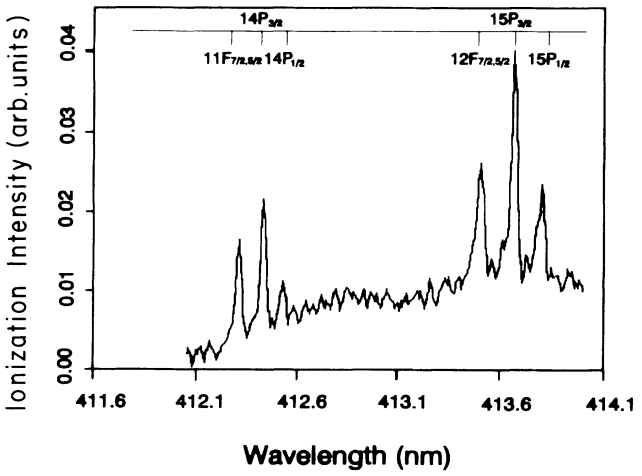

FIG. 1. A portion of REMPI spectra of the Tl atom fragmented from the photodissociation of TlI.

We can estimate the photon numbers involved in the photodissociation process by the simple formula $nh\nu \ge \sum_i E_i + E_d$. E_i indicates the term energy of the fragmented atoms and E_d, the dissociation energy of TlI. Since the threshold wavelength of photodissociation into the channel of $Tl^*(6\,^2P_{3/2})$ and $I(5\,^2P_{3/2})$ is $\sim$339 nm [10], the process of producing a $Tl^*(6^2P_{3/2})$ fragment upon irradiation at wavelengths >500 nm requires two-photon absorption. In this wavelength domain (500–600) nm, we have identified the nP, $8 \le n \le 12$ and nF, $5 \le n \le 9$ structures with $Tl^*(6\,^2P_{3/2})$ as the lower state of the ionization transition. The assignment is consistent with those results with the ground $Tl(6\,^2P_{1/2})$ fragment as the initial state in the related transition.

B. Spin-orbit coupling in the nP doublets

The results of spin-orbit splitting observed in the nP doublets are listed in Table III. Spin-orbit coupling mainly results from the interaction between the magnetic field of the circulating electron and the magnetic moment associated with the electron spin. For simplicity, we adopt a model suitable for a one-valence-electron, single-configuration condition. The related equation is given explicitly in the following [11,12]:

$$\Delta E_{1/2,3/2} = \langle \Psi_p | a(r)\mathbf{l}\cdot\mathbf{s} | \Psi_p \rangle = \alpha^2 \left[\frac{dn^*}{dn} \right] \frac{Z_a^2}{n^{*3}} \frac{Z_i^2 H_v \mathcal{R}}{l(l+1)(l+\frac{1}{2})} . \tag{3}$$

Here, α denotes the fine-structure constant, Z_i the effective nuclear charge, and H_v a relativistic correction. The value of H_v is almost unity for a light atom, but varies as an exponential-like function for the heavy atoms with atomic number $Z > 50$. Given an appropriate value of 1.2 for H_v adopted from Ref. [13], the best fit of simulation with Eq. (3) to the splitting observation of the nP doublets leads to a value of 75.4 for Z_i. We believe that our result is more precise than a previous value of 75, determined by taking into account only the lowest excited state [14]. The provision of Z_i is important in determining the hyperfine structure; its value for the Tl atom is on the order of 10^{-1} cm^{-1}, which cannot be resolved in this work.

To our surprise, as one can see in Table III, the simple model can be suitable for interpreting the spin-orbit splitting observed in the Tl nP doublets with an accuracy of $\pm 3.5\%$ except for $n=20$. The theoretical prediction in Table III is very consistent with our results, but slightly deviates from the data reported previously [3,9]. This fact may also confirm the reliability of our spectral assignment of the Rydberg states. Nevertheless, the model must be refined apparently to deal with the more complicated observation. A dedicated model, for instance, taking into account the exchange polarizability of the core electrons with the valence electron, has been employed successfully for interpreting the negative spin-orbit constant found in the Rb atom [15].

TABLE I. Term energy for $nP_{1/2}$, $nP_{3/2}$, and $nF_{5/2,7/2}$ Rydberg states of the Tl atom in units of cm^{-1}. The uncertainty is within $\pm 0.4\ cm^{-1}$.

	This work			Mirza and Duley [3]			Moore [9]		
n	$^2P_{1/2}$	$^2P_{3/2}$	$^2F_{5/2,7/2}$	$^2P_{1/2}$	$^2P_{3/2}$	$^2F_{5/2,7/2}$	$^2P_{1/2}$	$^2P_{3/2}$	$^2F_{5/2,7/2}$
5			42 321.8						42 318.4
6			44 824.0			44 823.5			44 823.5
7	34 159.4	35 163.0	46 188.3			46 185.7	34 159.9	35 161.1	46 185.3
8	41 375.3	41 749.3	46 972.6			47 004.6	41 368.1	41 740.8	47 004.6
9	44 379.4	44 562.3	47 535.3	44 381.0	44 567.5	47 539.1	44 380.9	44 562.5	
10	45 942.2	46 045.8	47 901.9	45 939.7	46 047.6	47 900.4	45 939.3	46 043.6	
11	46 859.3	46 921.9	48 159.1	46 854.4	46 920.9	48 161.8	46 853.8	46 917.1	
12	47 436.1	47 481.1	48 350.1	47 439.2	47 481.2	48 354.4	47 442.6	47 477.4	
13	47 833.2	47 862.9	48 499.0	47 832.6	47 862.7	48 501.0	47 847.7	47 847.7	
14	48 111.6	48 132.5	48 612.1	48 112.2	48 134.9	48 614.4	48 129.6	48 129.6	
15	48 315.0	48 330.2	48 702.1	48 320.4	48 337.4	48 703.4	48 331.2	48 331.2	
16	48 471.9	48 482.5	48 775.7	48 471.4	48 484.0	48 777.4	48 459.5	48 459.5	
17	48 590.9	48 600.3	48 837.9	48 590.7	48 600.6	48 835.4			
18	48 685.5	48 692.6	48 885.9	48 685.5	48 693.4	48 886.1			
19	48 761.5	48 767.4	48 921.9		48 768.9	48 927.1			
20	48 824.0	48 829.3	48 954.8		48 829.6	48 962.3			
21		48 878.3	48 989.6		48 880.4				
22		48 904.5							
23		48 947.6							

It is interesting to note that the intensity ratio of ionization transition via the respective intermediate $n\ ^2P_{3/2}$ and $n\ ^2P_{1/2}$ doublets behaves abnormally from the ratio of their statistical weights. As shown in Fig. 3, the $n\ ^2P_{3/2}$ to $n\ ^2P_{1/2}$ ratio of ionization intensity at $n \leq 14$ is smaller than 2, but becomes larger with increasing n. A similar result has been found in Rb, giving a ratio of 5.9 at large n [16]. The intensity ratio of Hg^+ $D_{5/2}$ to $D_{3/2}$ ionic states was also found to be 2.0 at 548 Å and 1.37 at 304 Å, showing discrepancy from 1.5 [17,18]. Such abnormal phenomena have been theoretically interpreted, for instance, by taking into account configuration interaction [19] or core polarizability exchange [20].

The intensity of ionization transition can be assumed to be a product of the transition probabilities between the first-step transition from the Tl $6\ ^2P_{1/2}$ (or $6\ ^2P_{3/2}$) to $n\ ^2P_{3/2}$ or $n\ ^2P_{1/2}$ intermediate state as well as the second-step transition from the $n\ ^2P_{3/2}$ or $n\ ^2P_{1/2}$ to continuum state. Since the relative intensity for the first-step transition depends upon the statistical weights of the nP fine-structure components, therefore, the abnormal intensity ratio observed above is subject to the dynamic variation of the matrix element related to the second-step ionization transition. The ionization transition probability, which is proportional to the photoionization cross section, can be expressed as $|\langle \Psi_\varepsilon | r | \Psi_p \rangle|^2$. The initial electronic wave function Ψ_p denotes the Tl $n\ ^2P_{3/2}$ or $n\ ^2P_{1/2}$ state; the final continuum wave function Ψ_ε denotes the

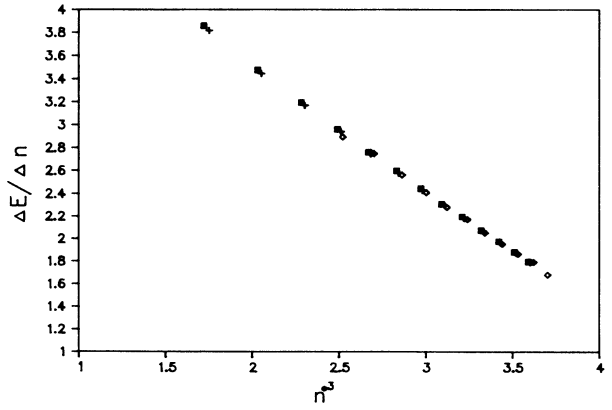

FIG. 2. Logarithmic plot of the n^{*3} dependence of $\Delta E/\Delta n$. ΔE indicates the term energy difference (in cm^{-1}) between two successive states. The symbol ■ indicates $n\ ^2P_{1/2}$, + indicates $n\ ^2P_{3/2}$, and ◇ indicates $n\ ^2F_{5/2,7/2}$ Rydberg states.

TABLE II. Effective principal quantum number n^* and quantum defect δ for $^2P_{1/2}$, $^2P_{3/2}$, and $^2F_{5/2,7/2}$ states.

	$^2P_{1/2}$		$^2P_{3/2}$		$^2F_{5/2,7/2}$	
n	n^*	δ	n^*	δ	n^*	δ
5					3.98	1.02
6					4.97	1.03
7	2.70	4.31	2.79	4.21	5.97	1.03
8	3.73	4.27	3.82	4.18	6.92	1.08
9	4.74	4.26	4.83	4.17	7.97	1.03
10	5.75	4.25	5.84	4.16	8.98	1.03
11	6.76	4.25	6.85	4.16	9.97	1.04
12	7.75	4.25	7.85	4.16	10.96	1.04
13	8.76	4.24	8.85	4.15	11.98	1.03
14	9.76	4.24	9.85	4.15	12.97	1.03
15	10.75	4.25	10.84	4.16	13.97	1.03
16	11.77	4.23	11.85	4.15	14.99	1.01
17	12.77	4.23	12.86	4.14	16.04	0.96
18	13.77	4.23	13.86	4.14	17.05	0.95
19	14.77	4.23	14.86	4.14		
20	15.78	4.23	15.89	4.12		
21			16.86	4.14		

TABLE III. Spin-orbit splitting in units of cm^{-1} for the $n\,^2P_{1/2,3/2}$ doublets. The experimental uncertainty is within $\pm 0.6\ cm^{-1}$.

	This work		Mirza	
n	Expt.	Cal.	and Duley [3]	Moore [9]
7	1003.6	1017.1		1001.2
8	374.0	374.9		372.7
9	182.9	182.3	186.5	181.6
10	103.7	102.2	107.9	104.3
11	62.7	62.0	66.5	63.3
12	45.0	41.8	42.0	34.8
13	29.8	28.7	30.1	
14	20.8	20.6	22.7	
15	15.2	15.7	17.0	
16	10.6	11.8	12.6	
17	9.4	9.3	9.9	
18	7.1	7.4	7.9	
19	6.0	6.1		
20	5.4	3.9		

kd or *ks* state in the ionization continuum region allowed by the selection rule. The dipole integral in the transition probability can be regarded roughly as an overlap between two radial components of the electronic wave functions. Cooper [21] has suggested that the overlap between the initial radial wave function of a discrete state and the final radial wave function of an ionic state can change as a function of the excess energy over the ionization threshold. When this excess energy becomes larger, the wavelength of the free-electron wave becomes smaller and then the corresponding continuum wave function will draw in closer to the nucleus [21]. If increasing the excess energy causes overlap enhancement between the initial and final radial wave functions, then the related photoionization cross section may rise with the excess energy, whereas the overlap cancellation of these two wave functions may lead to a decline of the photoionization cross section. The wave function of the valence electron for the $n\,^2P_{3/2}$ spin-orbit excited state is expected to be repelled slightly further from the nucleus with respect to the $n\,^2P_{1/2}$ state, and accordingly experiences the overlap with the continuum wave function of the ionic state prior to that of the $n\,^2P_{1/2}$ state. If the photoionization cross section associated with the nP state rises with the excess energy, that suggests the ionization transition intensity via the $n\,^2P_{3/2}$ intermediate state should experience enhancement prior to that via the $n\,^2P_{1/2}$ state, and accordingly the $n\,^2P_{3/2}$ to $n\,^2P_{1/2}$ ratio of ionization intensity becomes larger than their statistical-weights ratio. Analogously, a decrease for the photoionization-cross-section prediction as a function of the excess energy may explain the behavior of the intensity ratio smaller than 2. Such an interpretation has been successfully applied to the ionization-intensity ratio related to the subshell electron configuration, which can be probed by photoelectron spectroscopy [17,18].

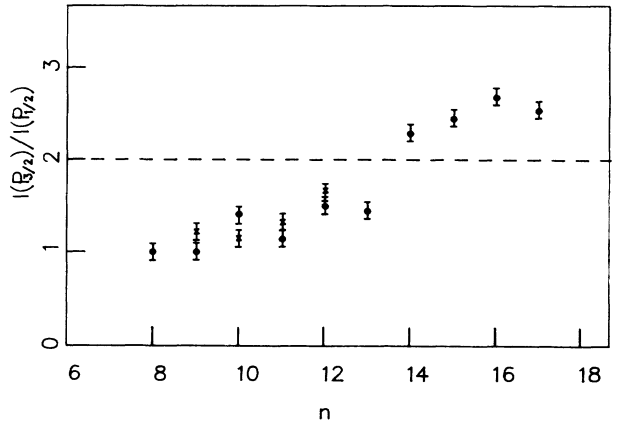

FIG. 3. The n dependence of the ionization intensity ratio via the intermediate $n\,^2P_{1/2}$ and $n\,^2P_{3/2}$ doublets. The symbol ● indicates that Tl ($6\,^2P_{1/2}$) is used as the lower state in the ionization transition, and × indicates that Tl ($6\,^2P_{3/2}$) is the lower state of the related transition.

In the following, we calculate the photoionization cross section of nP as a function of the excess energy using the quantum-defect method, which was first developed by Burgess and Seaton [22] and later modified by Peach [23]. The photoionization cross section can be expressed explicitly as follows [23]:

$$a_\upsilon = \frac{4\pi\alpha a_0^2}{3}\left[\frac{Z_a^2}{\upsilon}+Z_a^2\varepsilon'\right] \times \sum_{l'=l+1} C_{l'}\left|\int_0^\infty P_{\upsilon l}(r)\,r\,G_{k'l'}(r)\,dr\right|^2 , \quad (4)$$

where α is the fine-structure constant and a_0 is the Bohr radius. $P_{\upsilon l}(r)$ indicates the initial radial wave function of the bound state, and $G_{k'l'}(r)$, the final radial wave function of the continuum state. ε' denotes the energy (in units of rydbergs) of the ejected electron, which has angular momentum l', k' is defined to be $(Z_a^2\varepsilon')^{1/2}$, and Z_a is the charge of atomic core and equal to unity for neutral atoms. $\upsilon(=n^*)$ is the effective quantum number and is defined in Eq. (2). The coefficients $C_{l'}$ are related to the angular momentum and spin quantum number of the ini-

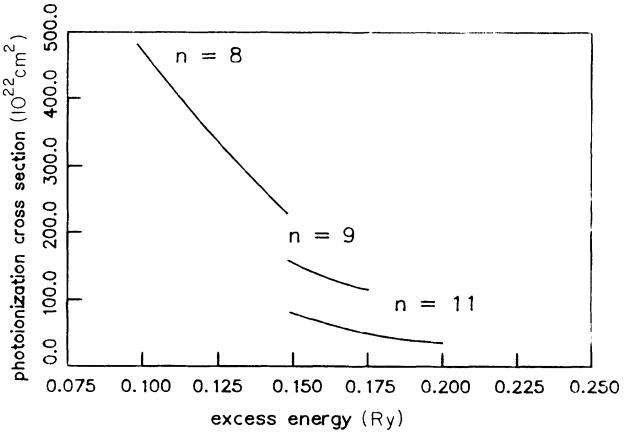

FIG. 4. Calculation of the photoionization cross section of the Tl $n\,^2P$ states ($n=8,9,11$) as a function of excess energy (in units of rydbergs) over the ionization threshold.

tial and final states. For calculation of these coefficients the reader is referred to Ref. [22]. According to Eq. (4), we follow the method developed by Peach [23] to calculate the photoionization cross section as a function of the excess energy. The result is shown in Fig. 4, revealing that the cross section decreases with increasing the excess energy, as $n \leq 11$. The fact is consistent with the interpretation described previously for the ratio smaller than 2. For large n ($n \geq 14$), however, we cannot satisfactorily apply this model for several reasons. First of all, the accuracy inherent in this model becomes very poor as the excess energy (or n) becomes large [22,23]. Second, the fine-structure splittings become so small about the order of 10 cm^{-1} for large n that the radial wave-function overlap between the respective fine-structure doublets and the ionization continuum hardly seems to resolve spatially. Thus interpretation with the concept described above becomes insignificant. Finally, as mentioned in the preceding section, the photoionization process no longer prevails for large n; the ionization mechanism may be partly contributed from the thermal ionization channel. Accordingly, it will be less significant with the photoionization cross-section prediction to account for the ionization ratio at large n.

In summary, using the REMPI technique, we have achieved identification of the $n\,^2P_{1/2}(7 \leq n \leq 20)$, $n\,^2P_{3/2}(7 \leq n \leq 23)$, and $n\,^2F_{5/2,7/2}(5 \leq n \leq 21)$ Rydberg states. We have also carried out a model calculation, which is consistent with the observation of spin-orbit splitting with an accuracy $\pm 3.5\%$. For small n, the $n\,^2P_{3/2}$ to $n\,^2P_{1/2}$ ratio of ionization intensity can be satisfactorily interpreted in terms of photoionization-cross-section prediction.

ACKNOWLEDGMENTS

The authors (K.C.L. and A.S.) wish to thank Professor J. R. Wiesenfeld for helpful discussions, as they have benefited greatly from his intelligent advice while working in his group. This work is supported in part by the National Science Council of the Republic of China.

*Author to whom correspondence should be addressed.

[1] R. F. Stebbings and F. B. Dunning, *Rydberg States of Atoms and Molecules* (Cambridge University, New York, 1983).
[2] S. Feneuille and P. Jacquinot, Adv. At. Mol. Phys. **17**, 99 (1981).
[3] M. Y. Mirza and W. W. Duley, Opt. Commun. **25**, 185 (1978).
[4] C. J. Smithells and E. A. Brandes, *Metals Reference Book*, 5th ed. (Butterworths, Boston, 1976).
[5] The photoabsorption cross section is $<5\times10^{-17}$ cm^2 for TlI, see P. Davidvovits and J. A. Bellisio, J. Chem. Phys. **50**, 3560 (1969).
[6] H. C. Chang, Y. L. Luo, and K. C. Lin, J. Chem. Phys. **94**, 3529 (1991).
[7] K. C. Wang, K. C. Lin, and W. T. Luh, J. Chem. Phys. **96**, 349 (1992).
[8] For a review on ionization mechanisms, see T. B. Lucatonto and T. J. McIlrath, Appl. Opt. **19**, 3948 (1980).
[9] C. E. Moore, *Atomic Energy Levels*, Natl. Bur. Stand. Ref. Data Ser., Natl. Bur. Stand. (U.S.) Circ. No. 35 (U.S. GPO, Washington, DC, 1971), Vol. III.
[10] M. Kawasaki, H. Litvak, and R. Bersohn, J. Chem. Phys. **66**, 1434 (1977).
[11] H. A. Bethe and E. E. Salpeter, *Quantum Mechanics of One- and Two-electron Atoms* (Plenum, New York, 1977).
[12] H. G. Kuhn, *Atomic Spectra* (Academic, New York, 1962).
[13] I. I. Sobelman, *Atomic Spectra and Radiative Tranditions* (Springer-Verlag, New York, 1979).
[14] R. G. Barnes and W. V. Smith, Phys. Rev. **93**, 95 (1954).
[15] T. Lee, J. E. Rodgers, T. P. Das, and R. M. Sternheimer, Phys. Rev. A **14**, 51 (1976).
[16] S. Liberman and J. Pinard, Phys. Rev. A **20**, 507 (1979).
[17] J. L. Dehmer and J. Berkowitz, Phys. Rev. A **10**, 484 (1974).
[18] T. E. H. Walker, J. Berkowitz, J. L. Dehmer, and J. T. Waber, Phys. Rev. Lett. **31**, 678 (1973).
[19] E. Fermi, Z. Phys. **59**, 680 (1930).
[20] D. W. Norcross, Phys. Rev. A **7**, 606 (1973).
[21] J. W. Cooper, Phys. Rev. **128**, 681 (1962).
[22] A. Burgess and M. J. Seaton, Mon. Not. R. Astron. Soc. **120**, 121 (1960).
[23] G. Peach, Mem. R. Astron. Soc. **71**, 13 (1967).